Nanoscale

COMMUNICATION

View Article Online
View Journal

Cite this: DOI: 10.1039/c7nr04215a

Received 13th June 2017,
Accepted 25th September 2017

DOI: 10.1039/c7nr04215a

rsc.li/nanoscale

MicroRNA detection at femtomolar concentrations with isothermal amplification and a biological nanopore†

Haolin Zhang, [a] Moe Hiratani,[b] Kentaro Nagaoka [a] and Ryuji Kawano *[b]

One of the greatest challenges faced by chemists and biologists is the detection of molecules at extremely low concentrations. This paper describes a method to detect ultra-low concentrations (1 femtomole) of nucleotides using isothermal amplification and a biological nanopore.

Nanopore sensing is a recent and emerging technology for the detection of single molecules, such as oligonucleotides, that can be translocated through a nanochannel of a pore-forming protein; it has also shown clear blocking currents at the single molecule level. Since Deamer and co-workers reported their pioneering work 20 years ago, extensive studies and applications, such as small molecule detection with adapters[1] or aptamers,[2] *in situ* mass-spectroscopy,[3] and nanopore sequencing, have been reported.[4,5] Furthermore, solid-state nanopores, rather than biological nanopores, have been developed by using an electron beam to form nanopores in silicon nitride[6] or graphene,[7] and other materials.[8–10] The biological nanopore alpha-haemolysin (αHL) is a toxin channel secreted by the bacterium *Staphylococcus aureus*, which has been mainly used as an oligonucleotide-detecting nanopore because the size of the pore is comparable to that of single-stranded (ss) DNA or RNA molecules.[11–15] Therefore, much effort has been exerted on using αHL nanopores for ssDNA detection in single DNA sequencing. In 2015, Oxford Nanopore Co. Ltd successfully released a portable sequencer using an other biological nanopore as a commercialized product; this will lead to the development of extensive practical applications in nanopore sensing.

One expected nanopore application is the detection of microRNAs (miRNAs), small non-coding RNAs composed of 20–30 nucleotides that are produced by two RNase III proteins, Drosha and Dicer.[16,17] Through RNA silencing and post-transcriptional regulation of gene expression, miRNAs are involved in various cellular processes, including differentiation, proliferation, migration and invasion. Accumulating evidence suggests that abnormal miRNA expression in tissues or blood is related to the development of cancer or other diseases.[18] As a result, the aberrant expression of miRNAs in serum or tissue has been suggested to have a diagnostic value for several diseases.[19–22] Generally, the methods used for miRNA detection, such as reverse transcription polymerase chain reaction (RT-PCR) and DNA arrays, are quite time-consuming. Several attempts at miRNA detection using nanopores have been recently reported,[23–26] indicating that the nanopore method is a promising candidate for simple and rapid miRNA detection. However, one of the most significant issues in the detection of miRNAs is their low (femtomolar) concentrations, especially during the early stages of cancer development. Therefore, the development of ultra-sensitive, simple, and rapid nanopore sensing methods would be of great significance.

To detect low concentration oligonucleotides using nanopores, two effective techniques have been previously proposed. The first is a physicochemical strategy based on the asymmetry of electrolytes between the *cis* and *trans* sides of the nanopore, enhancing the ionic flow through the nanopore. This flow enhances nucleotide translocation even at low concentrations. This method, using αHL, facilitated translocation at concentrations as low as 1 pM.[25] The second is an electrical strategy based on dielectrophoretic (DEP) force that is applied at the opening of a solid (glass) nanopore, which can enhance the oligonucleotide translocation. This method, using a glass nanopore, facilitated the translocation of dsDNA at concentrations as low as 5 fM.[27] In this study, we have attempted to achieve an even lower detection concentration, 1 fM, by combining oligonucleotide amplification and the asymmetric method described above. Based on these technologies, we attempted to measure 1 fM of miR-20a, which is secreted from lung cancer tissue.[28] We constructed this amplification system based on isothermal amplification[29,30] using miR-20a as the

[a]*Laboratory of Veterinary Physiology, Cooperative Department of Veterinary Medicine, Faculty of Agriculture, Tokyo University of Agriculture and Technology, Tokyo 183-8509, Japan*
[b]*Department of Biotechnology and Life Science, Tokyo University of Agriculture and Technology (TUAT), 2-24-16 Naka-cho Koganei-shi, Tokyo 184-8588, Japan. E-mail: rjkawano@cc.tuat.ac.jp*

†Electronic supplementary information (ESI) available. See DOI: 10.1039/c7nr04215a

input and poly-thymines as output molecules. Detailed information on the materials and methods is described in the ESI.† The amplified DNA from 1 fM concentration of miRNA could be measured by αHL nanopores under asymmetric conditions. This approach is a promising method for detecting miRNAs at ultra-low concentrations using nanopores (Fig. 1).

To achieve specific miR-20a amplification, the DNA template and primer were designed according to the miR-20a sequence as follows: DNA template, 5′-AAAAAAAAAAAAAAA-AAAAAAAAGATCCTTGTTTTGGAATAAGCACTTTA-3′; primer, 5′-CTACCTGCACTACCAAAA-3′; miR-20a, 5′-UAAAGUGCUUAU-AGUGCAGGUAG-3′. The DNA template and primer were partially complementary to miR-20a by 11 and 12 bp, respectively. As illustrated in Fig. 2, a three-way junction forms between the DNA template and primer in the presence of miR-20a. However, stable association is not expected to occur between the DNA template and primer in the absence of miR-20a, due to the limited number of complementary nucleotides and resultant low melting temperature. Following a three-way junction formation, the DNA polymerase Bst binds to the DNA template and elongates the complementary sequence using dNTPs as a substrate at 37 °C. A recognition site for the nicking enzyme Nt.AlwI was included in the DNA template, which is highlighted in yellow in Fig. 2B. The elongated complementary sequence is nicked by Nt.AlwI, which then initiates another cycle of DNA polymerization with the displacement of the single strand of polyT(20) (Fig. 2B). Therefore, polyT(20) is generated only in the presence of miR-20a.

To confirm the isothermal amplification reaction, we performed gel electrophoresis to detect the generation of polyT(20) with and without miR-20a (Fig. 3A, "+" and "−" lanes). The polyT(20) band is clearly visible in the presence of miR-20a, but not in its absence. This result suggests miR-20a-specific amplification of polyT(20).

The concentration of polyT(20) generated from isothermal amplification was measured using an asymmetric nanopore constructed from αHL for the ultra-sensitive detection of polyT (20), in accordance with a previous report that revealed increasing capture rates when an ionic gradient was established across the pore.[31] The 10-fold salt gradient was established across the nanopore by applying a 2 M KCl solution to the *trans* side and a 0.2 M KCl solution to the *cis* side. With the osmotic pressure and a 120 mV voltage between the *trans* and *cis* sides, we were able to measure the frequency of polyT(20) translocation from 1 to 1000 pM (Fig. 3B). The current blockade of polyT(20) was approximately 80% when translocation occurred, and other short current blockades also occurred due to collision (approximately 30%) and transient partial entry (approximately 60%).[32] A standard calibration curve was created based on the event frequency of >80% current blockades, shown in Fig. 3B. According to the capture rate theory of polymer translocation, the polyT(20) translated from the nanopore would be separated into three steps with diffusion, drift and translocation.[33] The electro-osmotic field would increase

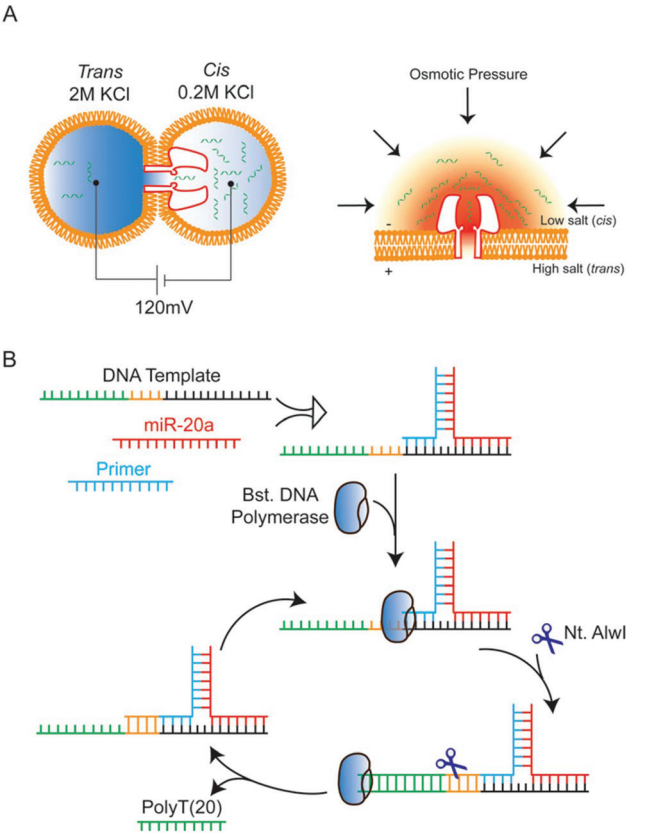

Fig. 2 (A) Schematic illustration of asymmetric nanopore detection for the generated polyT(20). (B) Schematic illustration of polyT(20) generation by isothermal enzyme reaction in the presence of miR-20a.

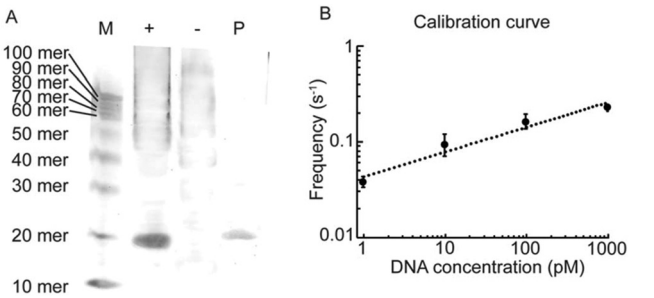

Fig. 3 (A) Gel electrophoresis of polyT(20) generation. M, size marker; +: with miR-20a (100 nM); −: without miR-20a. P: positive control. (B) The calibration curve of polyT(20) detection using the asymmetric nanopore.

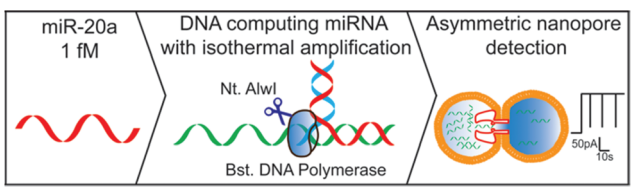

Fig. 1 Schematic diagram of miR-20a detection using DNA computing by isothermal amplification and asymmetric nanopore measurement.

the aggregation of polymers near the nanopore, where the capture rate was linear with the concentration of polymers.[33] After conquering the diffusion-limited regime, the polymers pass the energy barrier when successful translocation occurs.[31,33] Even under this asymmetric condition (2 M/0.2 M), the frequency of signature events was proportional to the DNA concentration, which was similar to those revealed in previous reports.[2,25]

The translocation frequencies of polyT(20) generated by isothermal amplification with or without miR-20a were also measured through the asymmetric nanopore (Fig. 4A). We measured the frequencies of polyT(20) translocation with 1 to 100 fM miR-20a after 1 hour of isothermal amplification, and the final concentration of polyT(20) generated from 1 fM miR-20a was 10.6 pM, which was calculated based on the calibration curve in Fig. 3B. The results suggest that 1 fM target miRNA can be adequately amplified and transformed into DNA molecules, which are more stable than RNA molecules. This high amplification may be partially due to the enzyme activity of the polymerase/nicking enzymes and the rapid amplification kinetics of isothermal reactions.[34,35] The detection limit could be extended to concentrations lower than 1 fM; however, this would require reaction optimization, including the types of enzymes used, their concentrations, and the reaction time. Using the other method of low concentration detection, a nanogap sensor demonstrated the sub-fM nucleotide detection of long mRNAs electrochemically;[36] however, this requires highly sophisticated microfabrications and may be limited for the detection of miRNAs due to their short length. There are several conventional methods for miRNA quantification, including real-time polymerase chain reaction (qRT-PCR), northern blot, and microarray analyses. Due to several limitations, such as their low sensitivity and specificity, as well as being time-consuming or expensive, the development of effective methods for miRNA detection is urgently needed.[37,38] Exponential isothermal amplification and nanotechnology represent a prospective method for miRNA detection. An obvious frequency elevation was observed with increased miR-20a concentration (Fig. 4A and B). The capture rate was 98 238 s^{-1} nM^{-1}, which was significantly higher than that of a conventional αHL nanopore (0.1 s^{-1} nM^{-1})[5] or a solid-state nanopore (263 s^{-1} nM^{-1}).[31] The *in vivo* miRNA concentration was in the fM range. Therefore, our method can detect specific miRNAs at fM concentration without labelling. In the future, we will study the ability of this method using a practical *in vivo* sample.

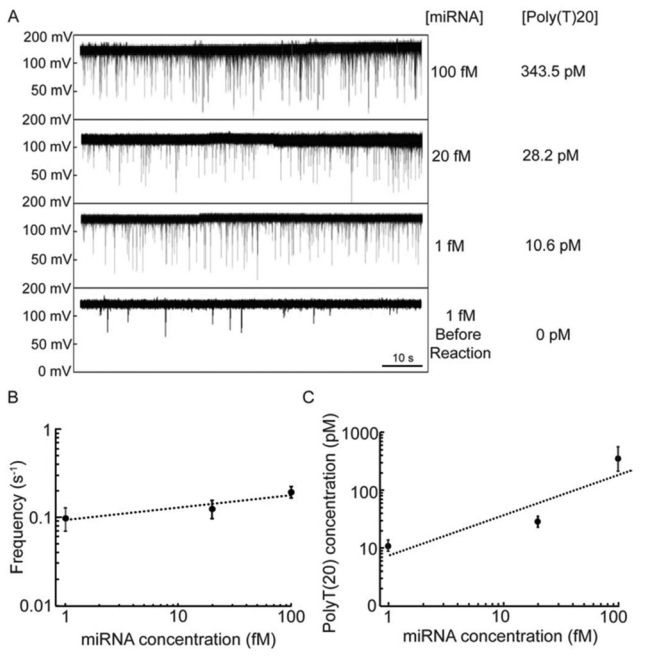

Fig. 4 (A) Typical current and time traces (1 min) of generated polyT (20) translocation in the asymmetric nanopore with different concentrations of miR-20a. (B) The capture rates of polyT(20) generated from different concentrations of miR-20a. (C) Correlation between miR-20a and polyT(20) concentrations.

Conclusions

In summary, we attempted ultra-low concentration miRNA detection by combining isothermal amplification and nanopore measurement. At miR-20a concentrations of 1 fM to 10 pM, stable DNA polyT(20) was transcribed and amplified. The output polyT(20) could be measured and quantified by nanopore measurement using the asymmetric solution method. The detection of 1 fM miRNA has been the lowest concentration detected by nanopore technology to date. Based on this methodology, by simply changing the nucleotide sequences of the DNA template and primer according to the target miRNA, different miRNAs can be specifically amplified. For practical application, the present method requires pretreatment, such as miRNA extraction, although the method does not require the condensation process. Additionally, the sensitivity of the present system may depend on the limitation of isothermal amplification. This system is potentially applicable for the diagnosis of any disease for which a diagnostic miRNA marker has been established.

Conflicts of interest

There are no conflicts of interest to declare.

Acknowledgements

This work was partially supported by KAKENHI (Grant No. 15H00803, 16H04226, and 16H06043) from MEXT, Japan.

Notes and references

1 H. Bayley and P. S. Cremer, *Nature*, 2001, **413**, 226–230.
2 R. Kawano, T. Osaki, H. Sasaki, M. Takinoue, S. Yoshizawa and S. Takeuchi, *J. Am. Chem. Soc.*, 2011, **133**, 8474–8477.

3 J. W. Robertson, C. G. Rodrigues, V. M. Stanford, K. A. Rubinson, O. V. Krasilnikov and J. J. Kasianowicz, *Proc. Natl. Acad. Sci. U. S. A.*, 2007, **104**, 8207–8211.
4 D. Deamer, M. Akeson and D. Branton, *Nat. Biotechnol.*, 2016, **34**, 518–524.
5 A. H. Laszlo, I. M. Derrington, B. C. Ross, H. Brinkerhoff, A. Adey, I. C. Nova, J. M. Craig, K. W. Langford, J. M. Samson, R. Daza, K. Doering, J. Shendure and J. H. Gundlach, *Nat. Biotechnol.*, 2014, **32**, 829–833.
6 N. Di Fiori, A. Squires, D. Bar, T. Gilboa, T. D. Moustakas and A. Meller, *Nat. Nanotechnol.*, 2013, **8**, 946–951.
7 S. Garaj, W. Hubbard, A. Reina, J. Kong, D. Branton and J. A. Golovchenko, *Nature*, 2010, **467**, 190–193.
8 B. M. Venkatesan, B. Dorvel, S. Yemenicioglu, N. Watkins, I. Petrov and R. Bashir, *Adv. Mater.*, 2009, **21**, 2771.
9 B. M. Venkatesan, J. Polans, J. Comer, S. Sridhar, D. Wendell, A. Aksimentiev and R. Bashir, *Biomed. Microdevices*, 2011, **13**, 671–682.
10 J. Larkin, R. Henley, D. C. Bell, T. Cohen-Karni, J. K. Rosenstein and M. Wanunu, *ACS Nano*, 2013, **7**, 10121–10128.
11 R. M. Manara, S. Tomasio and S. Khalid, *Nanomaterials*, 2015, **5**, 144–153.
12 L. Song, M. R. Hobaugh, C. Shustak, S. Cheley, H. Bayley and J. E. Gouaux, *Science*, 1996, **274**, 1859–1866.
13 A. F. Hammerstein, L. Jayasinghe and H. Bayley, *J. Biol. Chem.*, 2011, **286**, 14324–14334.
14 D. Japrung, M. Henricus, Q. Li, G. Maglia and H. Bayley, *Biophys. J.*, 2010, **98**, 1856–1863.
15 M. Ohara, Y. Sekiya and R. Kawano, *Electrochemistry*, 2016, **84**, 338–341.
16 D. P. Bartel, *Cell*, 2004, **116**, 281–297.
17 Y. Lee, C. Ahn, J. Han, H. Choi, J. Kim, J. Yim, J. Lee, P. Provost, O. Radmark, S. Kim and V. N. Kim, *Nature*, 2003, **425**, 415–419.
18 D. Hanahan and R. A. Weinberg, *Cell*, 2011, **144**, 646–674.
19 S. Alsidawi, E. Malek and J. J. Driscoll, *Int. J. Mol. Sci.*, 2014, **15**, 10508–10526.
20 B. D'Angelo, E. Benedetti, A. Cimini and A. Giordano, *Anticancer Res.*, 2016, **36**, 5571–5575.
21 M. Hubenthal, G. Hemmrich-Stanisak, F. Degenhardt, S. Szymczak, Z. Du, A. Elsharawy, A. Keller, S. Schreiber and A. Franke, *PLoS One*, 2015, **10**, e0140155.
22 K. Takahashi, I. Yan, H. J. Wen and T. Patel, *Clin. Biochem.*, 2013, **46**, 946–952.
23 L. Q. Gu and Y. Wang, *Methods Mol. Biol.*, 2013, **1024**, 255–268.
24 K. Tian, Z. He, Y. Wang, S. J. Chen and L. Q. Gu, *ACS Nano*, 2013, **7**, 3962–3969.
25 Y. Wang, D. Zheng, Q. Tan, M. X. Wang and L. Q. Gu, *Nat. Nanotechnol.*, 2011, **6**, 668–674.
26 X. Zhang, Y. Wang, B. L. Fricke and L. Q. Gu, *ACS Nano*, 2014, **8**, 3444–3450.
27 K. J. Freedman, L. M. Otto, A. P. Ivanov, A. Barik, S. H. Oh and J. B. Edel, *Nat. Commun.*, 2016, **7**, 10217.
28 H. Zhang, F. Mao, T. Shen, Q. Luo, Z. Ding, L. Qian and J. Huang, *Oncol. Lett.*, 2017, **13**, 669–676.
29 M. Hiratani, M. Ohara and R. Kawano, *Anal. Chem.*, 2017, **89**, 2312–2317.
30 Q. Zhang, F. Chen, F. Xu, Y. Zhao and C. Fan, *Anal. Chem.*, 2014, **86**, 8098–8105.
31 M. Wanunu, W. Morrison, Y. Rabin, A. Y. Grosberg and A. Meller, *Nat. Nanotechnol.*, 2010, **5**, 160–165.
32 M. Akeson, D. Branton, J. J. Kasianowicz, E. Brandin and D. W. Deamer, *Biophys. J.*, 1999, **77**, 3227–3233.
33 M. Muthukumar, *J. Chem. Phys.*, 2010, **132**, 195101.
34 T. Tian, J. Wang and X. Zhou, *Org. Biomol. Chem.*, 2015, **13**, 2226–2238.
35 K. Komiya and M. Yamamura, *New Generat. Comput.*, 2015, **33**, 213–229.
36 X. Chen, S. Roy, Y. Peng and Z. Gao, *Anal. Chem.*, 2010, **82**, 5958–5964.
37 E. Koscianska, J. Starega-Roslan, K. Czubala and W. J. Krzyzosiak, *Sci. World J.*, 2011, **11**, 102–117.
38 X. Zhang and Y. Zeng, *J. Visualized Exp.*, 2011, e3250, DOI: 10.3791/3250.

